

# An Improved Square-Root Nyquist Shaping Filter

fred harris  
San Diego State University  
[fred.harris@sdsu.edu](mailto:fred.harris@sdsu.edu)

Sridhar Seshagiri  
San Diego State University  
[Seshigar.@engineering.sdsu.edu](mailto:Seshigar.@engineering.sdsu.edu)

Chris Dick  
Xilinx Corp.  
[chris.dick@xilinx.com](mailto:chris.dick@xilinx.com)

Karl Moerder  
Broadband Innovations  
[kmoerder@broadbandinnovations.com](mailto:kmoerder@broadbandinnovations.com)

## Abstract

A Nyquist filter can have any odd symmetric taper as a transition between its pass band and stop band. The most well known taper is the raised cosine (RC) taper specified in most communication standards. The square root (SR-RC) Nyquist filter formed from this prototype exhibits high spectral side lobe levels that fail to meet severe spectral mask requirements. This paper presents a SR Nyquist filter with an alternate taper that, for the same length filter, achieves side lobe levels between one and two orders of magnitude below those obtained from a cosine tapered square root filter. This alternate filter also offers up to an order of magnitude reduction in residual ISI levels.

## 1. Introduction

The traditional RC tapered Nyquist spectrum is obtained by convolving the ideal rectangle spectrum of width  $1/T$  with a half cycle cosine shaped spectrum of width  $\alpha/T$ . The equivalent process seen in the time domain is the product of the two time series representing the inverse transforms of the rectangle and the half cycle cosine [1], [2] as is shown in (1).

$$h_{RC}(t) = \left(\frac{1}{T}\right) \frac{\sin(\pi \frac{t}{T})}{(\pi \frac{t}{T})} \frac{\cos(\pi \frac{\alpha}{T} t)}{[1 - (\frac{2\alpha}{T} t)^2]} \quad (1)$$

The (SR-RC) Nyquist spectrum [2], the spectral desired response for the shaping filter at the transmitter and of the matched filter at the receiver has the impulse response shown in (2).

The filters presented in (1) and (2) are symmetric about the time origin and have infinite extent. The realizable version of these filters is obtained by symmetrically truncating the time extent and then translating along the time axis till the response resides in the positive time interval. The truncation process is another time domain window that leads to a second spectral convolution which is the cause of high spectral side lobes exhibited by the SR-RC

Nyquist filter. We should know better than to simply truncate the impulse response of a filter!

$$h_{SR-RC}(t) = \left(\frac{1}{T}\right) \frac{(4\alpha \frac{t}{T}) \cos(\pi(1+\alpha) \frac{t}{T})}{(\pi \frac{t}{T}) [1 - (4\alpha \frac{t}{T})^2]} \quad (2) \\ + \left(\frac{1}{T}\right) \frac{\sin(\pi(1-\alpha) \frac{t}{T})}{(\pi \frac{t}{T}) [1 - (4\alpha \frac{t}{T})^2]}$$

Further when we convolve the truncated versions of the SR-RC Nyquist filters we do not obtain an RC-filter but rather an approximation that exhibits non-equally spaced zero crossings. The non-zero sample values taken at equally spaced sample positions are collectively the cause of non-channel induced inter-symbol interference (ISI).

## 2. Initial Design Procedure

Our task is to replace the standard SR-RC filter with one that does not suffer the defects related to the truncation or window applied to the impulse response of the prototype SR-RC filter. One successful approach to many filter designs involves variants of the Parks-McClellan (PM or Remez) algorithm that iteratively forms a weighted Chebyshev frequency domain approximation to the desired spectral response for a filter of specified length. The filter design requires a vector of frequencies identifying interval boundaries, a vector of gains at these frequency boundaries, and a penalty (or weight term) vector to control the tolerance bands about the desired response profile in each interval. Since we are considering an alternate transition in this design we are free to select any arbitrary odd symmetric transition shape and use the square root of that shape as the desired transition band response.

Rather than restrict the transition shape, we take a minimalist approach and specify three points in the transition band that the SR filter has to satisfy and permit the algorithm to acquire these points with the hope that the transition between these points will be well behaved. What ever

well behaved means! We know that the Nyquist filter gain at the half symbol rate is 0.5 (or -6 dB) hence the SR Nyquist filter gain at the half symbol rate is  $(0.5)^{1/2}$  (or -3 dB). As shown in figure 1, we require the spectral transition contour to pass through  $(0.5)^{1/2}$  at the bandwidth normalized frequency of 0.5.

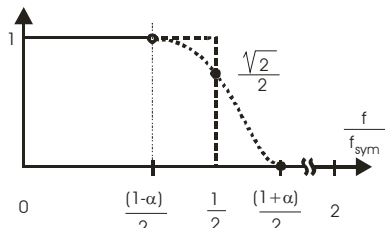


Figure 1. Frequency Response Specification for SR Nyquist Filter

We can accommodate this requirement a number of ways and here we employ an option of the PM algorithm [3], [4] that permits frequency intervals of zero width. The points we assign to the algorithm are the boundaries defining the pass band, the stop band, and the zero width interval in the transition band located between these two bands. These lead to the bandwidth normalized frequencies, gains, and weights shown in (3) for a filter designed with ratio of sample rate to symbol rate of 4. We will comment on the first weight, of value 2.4535, shortly.

$$\begin{aligned} \text{Freq } v: & [0 \quad (1-\alpha)/2 \quad 1/2 \quad 1/2 \quad (1+\alpha)/2 \quad 2]/2 \\ \text{Gain } v: & [1 \quad 1 \quad \sqrt{2}/2 \quad \sqrt{2}/2 \quad 0 \quad 0] \\ \text{Wt } v: & [2.4535 \quad 1 \quad 1 \quad 1] \end{aligned} \quad (3)$$

Figure 2 presents the log-magnitude spectral response of a 97-tap,  $\alpha = 0.2$ , SR-RC Nyquist filter and of a SR filter designed by the approach presented here. We refer to this option as the harris-Moerder-1 (hM-1) filter. Also seen here is a zoom to the in-band ripple detail. We first note and compare the -40 dB and -70 dB side lobe levels respectively of the SR-RC and of the hM-1 filters. This additional out-of-band spectral response is the goal of this design. We also note the 10-to-1 reduction of in-band ripple of the hM-1 filter relative to the SR-RC filter. The anomaly in the hM-1 filter is the 0.045 dB (or 0.5 %) spectral bump at the start of the transition band. This is the behavior we alluded to earlier when we hoped that the unrestricted spectral transition would be well behaved. We improve this behavior in the next section.

Figure 3 presents details of the inter-symbol interference (ISI) exhibited by a cascade of shaping and matched filters implemented as two SR-RC filters, as two hM-1 filters and as an hM-1 and an SR-RC filter. Here we note

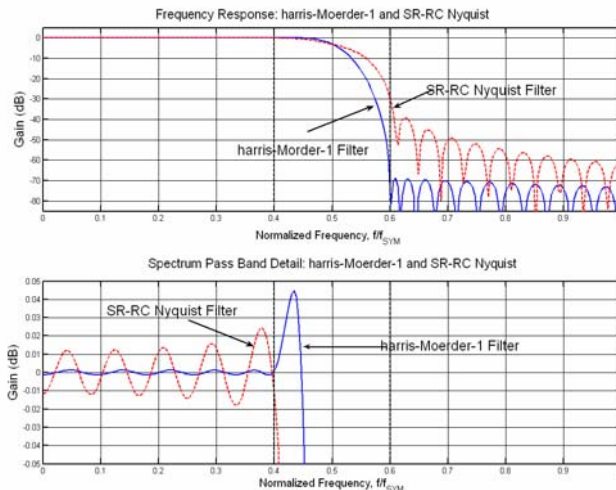


Figure 2. Spectrum and Pass Band Detail of SR-RC Nyquist and hM-1 Filters.

that the SR-RC and hM-1 filters exhibit RMS ISI levels of 0.41% and of 0.46% (-47.65 and -46.77 dB respectively) which are nearly comparable ISI levels for filters with very different spectral side lobe characteristics. What is interesting here is the ISI shown in the third subplot which presents the mismatch performance

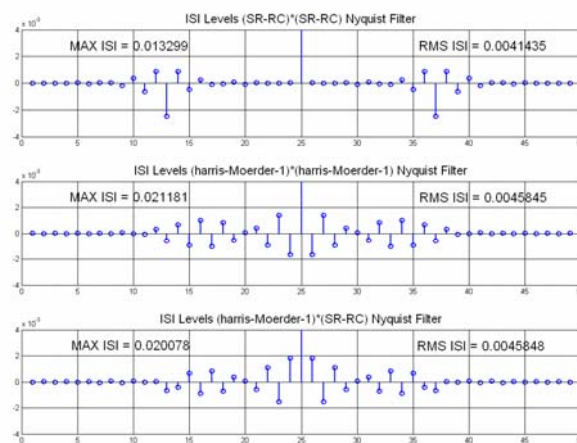


Figure 3. ISI levels of Matched SR-RC, hM-1 and of Mismatched SR-RC and hM-1 Filters

between filters at the modulator and the demodulator. This corresponds to the case in which we have selected the hM-1 filter at the transmitter to access its reduced spectral side lobe levels which faces a SQ-RC matched filter in a legacy receiver. We see here the same ISI levels for the hM-1 to hM-1 matched filter as for the mismatched hM-1 to SR-RC filters. This was not a remarkable coincidence but rather the result of adjusting the first weight in the PM algorithm weight vector shown in (3) to achieve this match.

### 3. Improved Design Procedure

The anomalous spectral bump at the edge of the transition band can be removed by redefining the pass band edge. The modified algorithm slides, in small increments, the pass band edge from  $(1-\alpha)/2$  to  $\beta(1-\alpha)/2$ . After each slide, the ISI obtained with the new filter weights is compared to the ISI obtained with the previous weights and the slide is continued till the ISI no longer decreases. Minimum ISI is obtained by a search refinement that iteratively reduces increment size and slide direction. The frequency vector used in the PM-algorithm is modified as shown in (4). Here  $\beta_2$  modifies the pass band edge to form a second set of weights hM-2 while  $\beta_3$  modifies the stop band edge to form a third set of weights hM-3.

$$\text{Freq } v: [0 \ \beta_2(1-\alpha)/2 \ 1/2 \ 1/2 \ \beta_3(1+\alpha)/2 \ 2]/2 \quad (4)$$

The ISI levels exhibited by matched filters hM-2 to hM-2 and by mismatched filters hM-2 to SR-RC are 0.062% and 0.62% (-64.2 and -44.2 dB respectively) while the ISI levels exhibited by matched filters hM-3 to hM-3 and by mismatched filters hM-3 to SR-RC are 0.037% and 0.52% (-68.6 and -45.7 dB respectively). For comparison, the ISI exhibited by the matched filter SR-RC to SR-RC is 0.41% (-47.65 dB). Figure 4 presents the log-magnitude spectral response for filter hM-3. Here we see the frequencies to which the two band edges have shifted to minimize its associated ISI.

Figure 5 presents details of the inter-symbol interference (ISI) exhibited by the cascade of shaping and matched filters implemented as two SR-RC filters, as two hM-3 filters and as an hM-3 and an SR-RC filter. As a matter of interest, figure 6 presents and compares the transition band edges of the spectra obtained at the output of the

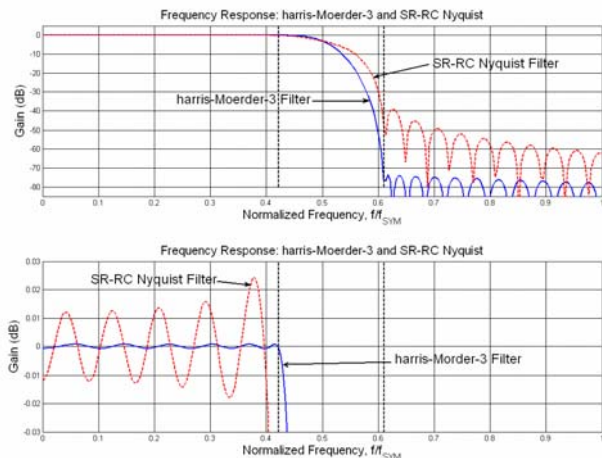


Figure 4. Spectrum and Pass Band Detail of SR-RC Nyquist and hM-3 Filters.

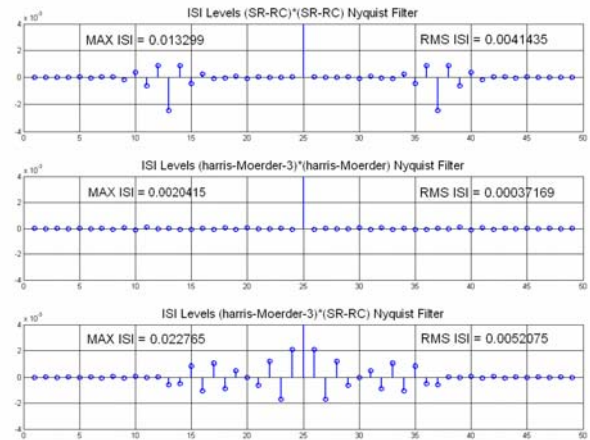


Figure 5. ISI levels of Matched SR-RC, hM-3 and of Mismatched SR-RC and hM-3 Filters

matched filter processing for the three filters we have examined, SR-RC, hM-1, and hM-3. Also shown are the spectral slopes for the three spectra. These are approximately the functions that are convolved with the ideal rectangle spectrum to form the finite duration, excess bandwidth SR Nyquist filter. The contour for the SR-RC is supposed to be an even symmetric half cosine. We clearly see the spectral distortion of the half cosine caused by time domain truncation. A pleasant observation is that the corresponding contour for the hM-3 filter is even symmetric. Finally we see the spectra formed by folding the out-of band spectrum back into band, an event that occurs when the output of the matched filter is sampled at symbol rate, one-sample per symbol. Ideally, these would all be constant unity level spectra and it the deviation from a constant that is responsible for the filter ISI.

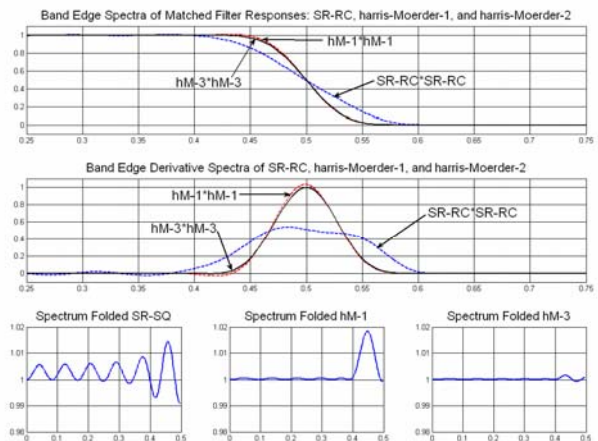


Figure 6. Transition Band Edge, Spectral Derivative, and Folded Spectra of SR-RC, hM-1, and hM-3 Filters

#### 4. Improving Mismatch Performance

The design technique we have been examining was formulated as a mechanism to obtain SR Nyquist filters with significantly reduced out of band spectral side lobes. This is accomplished by embedding a design with an unconstrained transition contour in the PM filter design algorithm. As expected, a filter with significantly improved out-of-band attenuation levels is characterized by a smoother transition between the pass band and stop band. We can see the smoother transition of the SR filters in figure 7 where the spectral derivative shows that the transition likely has many continuous derivatives. We note, by examining the spectral derivatives, that the hM filters have a narrower transition bandwidth than does the SR-RC. This, of course, is due to the zero derivatives at the boundaries of the transition bandwidth. We know that this difference in transition bandwidths will cause a mismatch between the shaped filter and the matched filter. As indicated earlier, this is a likely occurrence if an hM-3 filter is employed as a shaping filter at a new generation modulator which is processed by a SR-RC matched filter in a legacy receiver.

When we do the numbers, we find the mismatch loss is quite small. The inner product between the two mismatched signals, each normalized for unit energy, is 0.9978 or -0.0096 dB. We conclude that, in spite of the different transition contours, there is very little energy difference in the transition band. This suggests that we might be able to widen the transition bandwidth of the hM-3 shaping filter when we know that it is likely to be

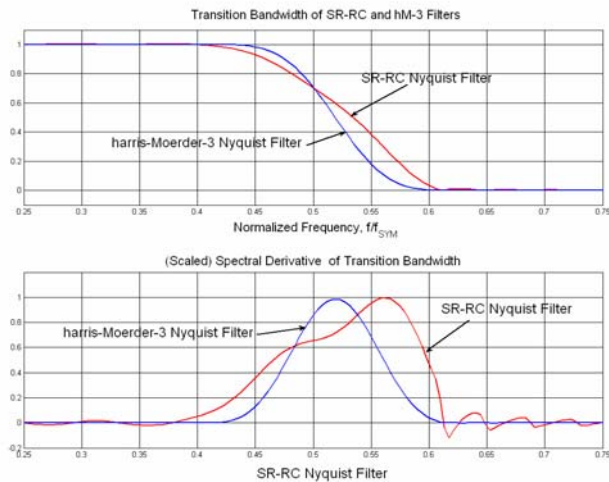


Figure 7. Detail of Transition Band Edge and Spectral Derivative of Band Edge of SR-RC and hM-3 Filters

used with a legacy SR-RC matched filter. We can do this with very little performance loss in collected energy but perhaps with the promise of improving ISI performance of the mismatched filters. In fact this proves to be true. To

illustrate the benefits of this option, we have designed hM filters with excess bandwidth of 0.21 for use as a shaping filter operating in conjunction with a legacy SR-RC filter with excess bandwidth 0.20.

Figure 8 presents details of the inter-symbol interference (ISI) exhibited by the cascade of these shaping and matched filters implemented as two SR-RC filters, as two hM-3 filters and as mismatched  $\alpha$  hM-3 and SR-RC filters. By adjusting the first weight term of (3) we were able to obtain the same RMS ISI level for all 3 filter pairings. Hence by permitting a minor  $\alpha$  mismatch between the hM shaping filter and the legacy SR-RC matched filter we incur no performance penalty while accessing the improved out-of-band spectral response of the hM filters. Figure 9 shows the spectra of the  $\alpha$ -mismatched filter pair. The anomalous 0.04 dB bump in the transition band is removed in the hM-2 and hM-3 versions of this  $\alpha$

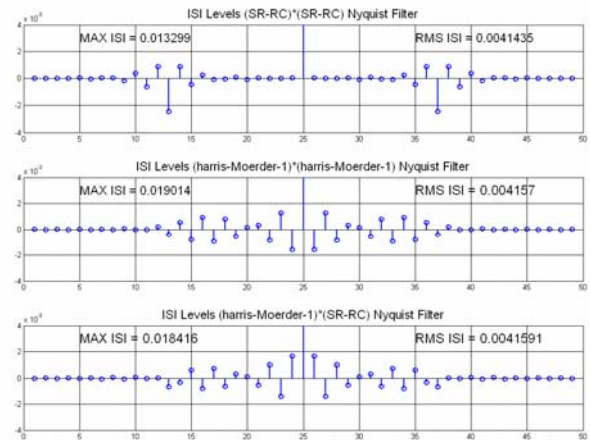


Figure 8. ISI levels of Matched SR-RC, hM-3 and of Mismatched  $\alpha$  SR-RC and hM-1 Filters

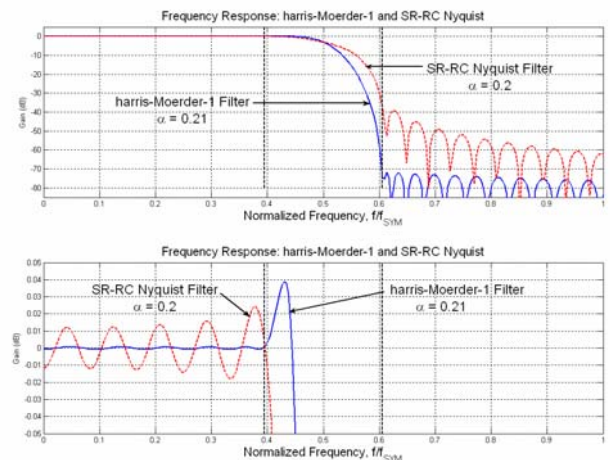


Figure 9. Spectrum and Pass Band Detail of  $\alpha$  Mismatched SR-RC Nyquist and hM-1 Filters.

mismatched filter. The bump free hM-3 version of this filter exhibits an improved matched filter RMS ISI level of 0.00072 (-62.9 dB) but has a reduced  $\alpha$  and shape mismatched filter RMS ISI level of 0.0054 (-45.4 dB). This compares to the SR-RC Nyquist RMS ISI level of 0.0041 (-47.7 dB).

Figure 10 presents the eye diagrams formed from the time series at the output of the hM-3 and SR-RC Nyquist matched filters. These are seen to be quite similar but the hM filter pair has slightly narrower width eye-opening and slightly larger peak transitions as expected for the its narrower effective transition bandwidth. We expect that this minor variation will not impact timing recovery loops when an hM shaping filter is substituted for the SR-RC filter.

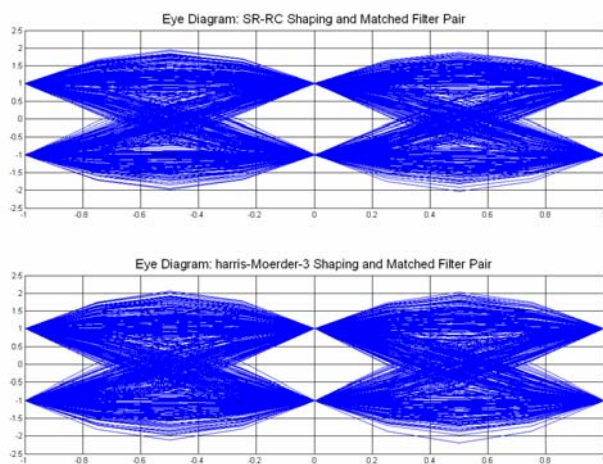


Figure 10. Eye Diagrams for SR-RC and hM-3 Shaping and Matched Filter Pairs

## 5. Conclusions

We have examined a design technique based on use of the PM-algorithm to form SR Nyquist filters with unconstrained transition contours that exhibit significantly reduced out-of-band side-lobe levels. One variant of this

design, hM-1, exhibits a small spectral bump at the starting edge of the transition band. The amplitude of this bump is approximately the magnitude of the in-band ripple exhibited by the standard SR-RC Nyquist filter. By adjusting the weighting term in the PM filter design algorithm we were able to obtain the same ISI level in the matched hM-1 to hM-1 filter pair as in the mismatched hM-1 to SR-RC Nyquist filter pair.

The spectral bump in the transition band is suppressed by shifting the pass band edge towards the transition band while monitoring the ISI performance of the corresponding time domain filter. This variant, denoted hM-2 and its shifted right band edge cousin, denoted hM-3 exhibit considerably reduced ISI levels. While the hM-2 and hM-3 matched filter pairs exhibit improved matched filter performance they also exhibit slightly reduced performance levels when mismatched with SR-RC Nyquist filters.

We suggested and demonstrated the use of a small intentional excess bandwidth ( $\alpha$  value) mismatch between the hM filter and legacy SR-RC Nyquist filters. This option offer the ability to use the hM filter, with its improved spectral characteristics, at a modulator without incurring a mismatch performance loss when used with SR-RC Nyquist filters residing in legacy receivers.

## 6. References

- [1]. John Proakis, "Digital Communications", Fourth Edition, 2001, McGraw-Hill, Ch. 9.2, pp. 554-561.
- [2]. fred harris, "Multirate Signal processing for Communication Systems", 2004, Prentice-Hall, Ch. 4.1-4.4, pp. 82-97
- [3]. Sanjit Mitra and James Kaiser, "Handbook for Digital Signal processing", 1993, John Wiley & Sons, Ch. 4.8, pp. 198-214
- [4]. MATLAB, FIRPM.m script file help response.